Does the Iron K_{α} Line of Active Galactic Nuclei Arise from the Cerenkov Line-like Radiation?

J. H. You[1,2], D. B. Liu[1], W. P. Chen[3], L. Chen[1], S. N. Zhang[4,5,6]

[1]*Institute for Space and Astrophysics, Department of Physics, Shanghai Jiao-Tong University, Shanghai, 200030, China, P. R.*

[2]*jhyou@online.sh.cn*

[3]*Institute of Astronomy and Department of Physics, National Central University, Chung-Li, 32054, Taiwan, China*

[4]*Center for Astrophysics, Physics Department, Tsinghua University, Beijing, 100084, China, P. R.*

[5]*Physics Department, University of Alabama in Huntsville, Huntsville, AL 35899, USA*

[6]*National Space Science and Technology Center, 320 Sparkman DR., SD50, Huntsville, AL 35805, USA*

ABSTRACT

When thermal relativistic electrons with isotropic distribution of velocities move in a gas region, or impinge upon the surface of a cloud that consists of a dense gas or doped dusts, the Cerenkov effect produces peculiar atomic or ionic emission lines — the Cerenkov line-like radiation. This newly recognized emission mechanism may find wide applications in high-energy astrophysics. In this paper, we tentatively adopt this new line emission mechanism to discuss the origin of iron K_{α} feature of AGNs. Motivation of this research is to attempt a solution to a problem encountered by the "disk-fluorescence line" model, i.e. the lack of temporal response of the observed iron K_{α} line flux to the changes of the X-ray continuum flux. If the Cerenkov line emission is indeed responsible significantly for the iron K_{α} feature, the conventional scenario around the central supermassive black holes of AGNs would need to be modified to accommodate more energetic, more violent and much denser environments than previously thought.

Subject headings: radiation mechanism: general — line: formation — X-rays: galaxies — Seyfert — black hole physics

1. Introduction

Observations in the last decade show that many active galactic nuclei(AGNs), e.g. the Seyfert 1 galaxies, display in their spectra an emission feature peaked around $\sim 6.4 - 6.5 \text{KeV}$, commonly attributed to the K_α line emission of iron ions in low- or intermediate-ionization states. The observed K_α line is very broad, and the line profile is asymmetric, being steep on the blue and flattening on the red wavelength wing, extending to $4 - 5 \text{KeV}$, as shown in Fig. 1 (Tanaka et al. 1995; Nandra et al. 1997a, 1997b; Fabian et al. 2002; Wang et al. 2001). The iron K_α is regarded as one of the best probes to explore the physical mystery in regions proximate to the central supermassive black holes of AGNs. Its observation and interpretation thus have drawn great attention lately in black hole and AGN study.

So far the prevailing model is based on the "photoelectric absorption-fluorescence line emission" mechanism (e.g.,Guilbert et al. 1998; Lightman et al. 1998; Fabian et al. 1989; Reynolds 2001), which has gained wide popularity because it successfully produces a line-profile consistent with observations. Furthermore, the underlying emission mechanism, that is, photoelectric absorption followed by fluorescence line emission, has been so far taken for granted as the only way to produce the X-ray atomic or ionic emission line by heavy ions in low- or intermediate-ionization states for which the K-shell of ion is fully filled. Take an iron ion as an example, because the K-shell is fully closed, so the transition $n = 2 \to 1$ (K_α) cannot occur unless certain external X-ray illumination causes photoelectric absorption to first make a "vacancy" in the K-shell.

Despite the success of the "photoelectric absorption-fluorescence line" mechanism, we suggest an alternative mechanism—the Cerenkov line-like radiation—to explore the origin of iron K_α in AGNs. The motivation of this research is to attempt a solution of a problem encountered by the "disk-fluorescence line" model, i.e. the temporal response of the iron K_α line flux to the changes of the X-ray continuum flux, predicted by a simple "photoelectric absorption-fluorescence line emission" model. So far no clear response of line flux to the incident X rays has been observed (e. g. Lee et al. 1999, 2000; Chiang et al. 2000; Wang et al. 1999, 2001; Weaver et al. 2001). It has been suggested that a flux-correlated change of ionization states of the iron ions would be responsible for the lack of correlation between the fluxes of iron K_α line and the continuum (e.g. Reynolds 2001). This may well be true, and deserves to give a further quantitative analysis to confirm this viewpoint. There is another model that attempts to explain the lack of temporal response. Vaughan & Fabian (2002) and Miniutti et al. (2003) suggest a model in which the X-ray source is close to the spin axis of the black hole, and the long-time scale changes (> 10 ks) are due to changing height of this source. The light bending effect can then produce an almost constant line intensity together with a changing observed continuum flux. In this paper, we try to give another explanation for this problem by use of the newly recognized Cerenkov line emission mechanism.

In sec. 2 of this paper, we first outline the physics of the new line emission mechanism to help people who are unfamiliar with this mechanism. Relevant basic formulae are presented in Appendix. Besides, we discuss the conditions under which the new emission mechanism become predominant over the photoionization-fluorescence process, and should be taken into consideration to explore the origin of the iron K_α line in AGNs. In sec. 3 we give some model considerations and model calculations by use of the new mechanism to match the observed luminosities of the iron K_α line, and in turn to see whether the estimated environmental parameters are reasonable and acceptable in regions proximate to the central supermassive black hole of AGNs. Sec. 4 is conclusions and discussions.

2. Cerenkov line-like radiation as the responsible mechanism—Outline of physics of the new mechanism

In this paper we propose that the "Cerenkov line-like radiation" (You et al. 2000, 1980, 1986) could be responsible for the iron emission feature in AGNs. We shall show that this emission mechanism may become predominant over the fluorescence process under certain conditions around AGNs. Furthermore, the possible difficulty encountered by the fluorescence mechanism as mentioned above, namely the lack of correlation between the line and the continuum fluxes, can be alleviated because the radiation energy of Cerenkov line is provided by relativistic electrons rather than by the X-ray continuum as in fluorescence process.

The Cerenkov line-like mechanism has been confirmed by elegant laboratory experiments in O_2, Br_2 and Na vapor using a ^{90}Sr β-ray source with the fast coincidence technique (Xu et al. 1981, 1988, 1989). Detailed discussions on the basic physics and improved formulae have been further presented recently (You et al. 2000, hereafter Y00). Here we outline the physics and essential results of the theory to help the people who are unfamiliar with this new mechanism. The relevant basic formulae are presented in Appendix of this paper for people who are interested in the theory of Cerenkov line-like radiation.

When the thermal relativistic electrons with isotropic distribution of velocities move in a gas region, or impinge upon the surface of a dense cloud with arbitrary shape (e.g. with filamentary or sheet-like structure), Cerenkov radiation is produced within a narrow wavelength range $\Delta\lambda$, very close to the intrinsic atomic or molecular wavelength λ_{lu} (u and l denoting respectively the corresponding upper and lower energy levels) because only in this narrow band the refractive index of gas is significantly larger than unit, $n > 1$, which makes it possible to satisfy the Cerenkov radiation condition $n \geq \frac{c}{v} \equiv \frac{1}{\beta}$. The emission feature therefore appears more like an atomic or molecular line than a continuum, thus the name "Cerenkov line-like radiation", or simply "Cerenkov emission line".

For gaseous medium, the dispersion curve $n \sim \lambda$ and the resonant line-absorption curve $\kappa \sim \lambda$ can be calculated exactly by use of the formula of the refractive index for gas, $\frac{\tilde{n}^2-1}{\tilde{n}^2+2} = \frac{4\pi}{3}N\alpha$, where

$\tilde{n} = n - i\kappa$ is the complex refractive index, with the real part n being the refractive index of gas, and the imaginary part κ being the extinction coefficient which relates with the line-absorption coefficient by a simple formula $k_{lu} = \frac{4\pi\nu}{c}\kappa_\nu$ (Y00, or eq. (13) in Appendix); N is the number density of the atomic/molecular species; α is the polarizability per atom or ion, given by quantum theory (Y00). For a very dense gas, n is large. For $\lambda \approx \lambda_{lu}$, the value of α, and hence the value of n, becomes very large (see the schematic dispersion curve $n^2 \sim \lambda$ in FiG. 2). We emphasize that $n > 1$ at $\lambda \gtrsim \lambda_{lu}$ validates even when the lower energy level l is fully closed, as long as the upper level u is not completely filled (see Eq. (11) in Appendix). This is substantially different with the fluorescence emission, which always requires to preempt a vacancy in the lower level. It is this unique property that makes it easier to produce the K_α line of iron ions in intermediate-ionization states by the Cerenkov mechanism, under certain circumstances, than by the fluorescence process.

In FiG.2 we see a strong resonant absorption occurs at $\lambda = \lambda_{lu}$ where the Cerenkov radiation vanishes. The Cerenkov mechanism only operates in the narrow shaded region $\lambda > \lambda_{lu}$, where the absorption approaches zero, $\kappa_\lambda \to 0$. The combination of absorption and emission causes the final emission feature slightly redshifted, which we call "Cerenkov line redshift" in order to distinguish it from other types of redshift mechanisms (Doppler, gravitational, Compton, etc.). As we shall show below, the Cerenkov line redshift is favorable to increase the emergent flux of Cerenkov emission line from the surface of a dense cloud.

In summary, the Cerenkov line-like emission has the following characteristics: (1) It is concentrated in a small wavelength range, so appears more like a line than continuum. The denser the gas, the broader the emission 'line' feature. (2) If the dense gas is optically thick for the Cerenkov line emission, the emergent line profile becomes asymmetric, being steep on the high energy side and flattened on the low energy side. (3) The peak of the emission feature is not exactly at $\lambda = \lambda_{lu}$ but slightly redshifted due to the line absorption shown in FiG.2. In the optically thick case, the typical value of 'Cerenkov line redshift' would be so high as $z \sim 10^{-3}$ (Y00), which in terms of Doppler effect would correspond to an apparent velocity of several hundred kilometers per second. (4) The radiation would be polarized if the relativistic electrons have an anisotropic velocity distribution.

FiG.3 shows the calculated profile of the Cerenkov K_α line of Fe^{+21} in optically thick case. For comparison a normal line by a spontaneous transition $n = 2 \to 1$ of Fe^{+21} ion is also shown in FiG.3 . The differences are obvious.

The redshift effect(item 3 above) conveniently provides a mechanism in favor of the emergence of Cerenkov line emission, particularly from dense clouds. Obviously, for an opaque, optically thick dense gas, the emergent line flux from the surface of cloud is determined by the competition between emission and absorption. The absorption mechanism for a Cerenkov line is drastically different from that for a normal line. A normal spectral line, exactly located at $\lambda = \lambda_{lu}$, would

be greatly weakened by a strong resonant line-absorption because the line absorption coefficient $k_{lu}(\lambda = \lambda_{lu})$ at $\lambda = \lambda_{lu}$, is very large(Fig. 2). In case of a very dense gas, the emergent radiation simply becomes a black-body continuum, and the normal line vanishes. In contrast, a Cerenkov line, occurs at $\lambda > \lambda_{lu}$ owing to the Cerenkov redshift, can avoid the strong line absorption because $k_{lu}(\lambda > \lambda_{lu}) \rightarrow 0$ (FiG. 2). Therefore a Cerenkov line suffers only very small amounts of photoelectric absorption $k_{\rm bf}$ (the extremely weak free-free absorption $k_{\rm ff}$ in X-ray band can be neglected), much smaller than the regular line absorption $k_{lu}(\lambda_{lu})$, i. e. $k_{\rm bf} \ll k_{lu}(\lambda = \lambda_{lu})$. For example, for the iron K_α line, the dominant photoelectric absorption comes from the L-shell electrons of iron ions, for which the photoelectric absorption coefficient $k_{\rm bf} \approx k_{\rm bf}({\rm Fe, L})$ is much smaller than the regular line absorption. That is, $k_{\rm bf} \approx k_{\rm bf}({\rm Fe, L}) \ll k_{lu}(\lambda = \lambda_{lu})$. This means that the photons of Cerenkov line can escape readily from deep inside a dense gas cloud; in other words, the dense gas would appear more 'transparent' for the Cerenkov line emission than for a normal line produced by the spontaneous transition. It is probable that the optical depth of a dense cloudlet with size r can be less than unit, $\tau = k_{\rm bf}({\rm Fe, L})r < 1$, despite of the high density of iron ions $N_{\rm Fe}$, i. e. the dense cloudlet possibly becomes optically thin for the peculiar Cerenkov line emission. Even if in the optically thick case, $\tau = k_{\rm bf}({\rm Fe, L})r > 1$, the Cerenkov emission layer at the surface of dense cloud with thickness $l \sim 1/k_{\rm bf}({\rm Fe, L})$ would still be surprisingly thicker than that for normal line. An optically thin case or a thick Cerenkov emission layer at the surface of an opaque dense gas region means a possibility of very strong emergent Cerenkov line emission, as long as there are sufficient number of relativistic electrons near the surface. It is possible that the Cerenkov line emission is even predominant over the markedly suppressed normal fluorescence line in such special cases.

3. Model considerations and calculations

3.1. Model considerations — new scenario As mentioned above, The Cerenkov line-like radiation may be particularly important in astrophysical environments with a very high gas concentration and with abundant relativistic electrons. One such example would be AGNs, particularly the Seyfert 1 galaxies, for which the existence of dense gas region seems plausible. The gas at the surface of an AGN disk is thought to be compressed to very high density by the high radiation pressure of the coronal X rays. However, although the disk-type geometry is compatible with the Cerenkov mechanism, in the following model consideration, we prefer to adopt the quasi-spherical distribution of dense cloudlets with spherical, filamentary or sheet-like shapes around the central black hole, in order to avoid some defiances on the validity of disk models (Sulentic et al. 1998a;1998b). The possible presence of such dense clouds, filaments and sheets in AGN environments has been discussed by Rees(1987);Celotti, Fabian & Rees(1992); Kuncic, Blackman & Rees (1996); Kuncic, Celotti & Rees (1997) and Malzac (2001). The clouds must be very dense to remain cool and therefore held by magnetic fields. Cool gas trapped by the magnetic field is compressed to extreme densities by the high radiation pressure, as what happens at the surface of disk surrounding the central supermassive black hole. Recently some

authors adopt the quasi-spherical distribution of dense cloudlets to explain the origin and profile of the iron K_α line (Karas et al. 2001; Collin-Souffrin et al. 1996; Brandt et al. 2000). In their scenario, the innermost part of the disk is disrupted due to disk instabilities. Part of the disrupted material forms the optically thick, cold cloudlets of dense gas that cover a significant portion of the sky from the point of view of the central X-ray source, while the rest gets heated up to high temperatures, forming a corona (see FiG.4). Recent observations support the existence of dense clouds or filaments in AGNs (Boller et al. 2002) which strongly favors the operation of Cerenkov line-like radiation mechanism.

FiG.4 sketches the schematic of our working model of a quasi-spherical emission region around the central supermassive black hole of a AGN. In FiG.4 the shaded spots or stripes represent cool cloudlets or filaments of dense gas. The dotted region stands for the hot, rarefied corona. The tiny dots, uniformly distributed in corona, represent thermal electrons and the black dots represent the relativistic electrons, which are highly concentrated around the cloudlets in corona (reasons see below).

Evidence also seems to be mounting on the existence of abundant relativistic electrons. It is likely that the observed power-law continuum over a very wide frequency range, from radio to UV is largely attributed to non-thermal radiation of relativistic electrons.[1] Although the detail mechanism to produce an excessive amount of high energy electrons remains unclear, flare events or some shock processes in corona may be responsible. Such shock processes also take place in the gamma-ray burst events, in which ultra-fast electrons are produced by the internal and external shock waves, thus producing the nonthermal radiation. The strong shock waves originate from drastic release of gravitational energy during the mergers processes, e. g. the neutron star-neutron star or the neutron star-black hole mergers (Piran 1999, 2000; Meszaros 2002). It is probable that similar processes also occur in AGNs environments. The biggest difference between the accretions of the AGNs supermassive black hole and the small black hole with solar mass could be that the accreted matter moving around the AGNs black hole is not in a pure gas state. Many components could be coexistent and mixed in regions proximate to the central black hole. Except of the dense cloudlets, there exist the solid debris and fragments, the meteorites and planets, even the stars, e. g. the neutron stars and the black holes with star mass. The frequent collisions and mergers between these objects should be expected, e. g. the mergers of meteorite-neutron star and mergers of planet-black hole, etc., which also produce a chain of 'merger-drastic release of gravitational energy-strong shock-plenty of fast electrons', though the scale of energy release in each merger could be much smaller than that in GRBs. Given the ubiquity of shock events in corona region around the central supermassive black hole, and their frequent collisions with dense clouds, the whole region of iron line emission is regarded as a shock-filled X-ray source(FiG.4). The collisions convert part of the kinetic energy of shock wave to thermal energy of relativistic electrons (see, e.

---

[1]However, there is no clear evidence for X-ray emission from highly relativistic electrons in Seyfert galaxies.

g. Piran 1999). Obviously most fast electrons thus produced are concentrated in a narrow zone which closes to the collision-front at the surface of the dense cloudlet (or on the flare spots if they are produced in flare events), as shown in FiG.4. Diffusion of fast electrons outward to ambient space is expected to be slow owing to the trapping effect of magnetic fields near the clouds or flares. The ability to retain extremely high concentration of relativistic electrons near the dense clouds undoubtedly provides a very favorable environment for the operation of the Cerenkov line emission.

If the conditions, namely the existence of dense gas and relativistic electrons, are met, the Cerenkov line like emission becomes inevitable.

3.2. Model calculation   Now we derive the intensity or luminosity of the Cerenkov line, in particular the iron K_α line, under various environmental parameters, and compare it with observations. Except for the geometric size of emission region, the main factors that determine the luminosity of the Cerenkov line include the density of the iron ions N_{Fe}, the density of the relativistic electrons N_e, and the average or typical energy γ_c of the relativistic electrons, where the Lorentz factor $\gamma \equiv \frac{1}{\sqrt{1-\beta^2}} = \frac{mc^2}{m_0 c^2}$ represents the dimensionless energy of an electron in unit of $m_0 c^2$. Our goal is to estimate the (range of) values of N_e, N_{Fe} and γ_c under a fixed size D of emission region from the theory of Cerenkov line radiation(Y00), to match the observed luminosities of the iron K_α line, and in turn to see whether these values are acceptable in the environment of AGNs.

In this paper, our main interest is in the energetics of the iron K_α emission process, therefore we leave out lengthy discussion on the line profile, except to note that even though a Cerenkov line is intrinsically broad, asymmetric and redshifted, it is still insufficient to produce the highly skew emission features observed in AGNs. A supermassive black hole is still needed to provide the necessary Doppler broadening and gravitational redshift.

We assume a typical mass $M \sim 10^{7-8} M_\odot$ for the central black hole. From the observed variation time scales of the iron K_α line (~ 1 lt day, see Nandra, George, Mushotzky, et al. 1997; Done et al. 2000), we infer the size of the emission region to be $D \sim 10^{15-16}$cm. In the following model calculations, we adopt a typical value $D \approx 3 \times 10^{15}$cm, or about $\sim 10^{2-3} R_{Sch.}$, where $R_{Sch.}$ is the Schwarzschild radius. To simplify the calculation, we assume all of the dense gas regions in the form of spherical cloudlets with the same radius, except to note that in reality they will naturally be in various cloud-like, filament-like or sheet-like shapes with various sizes. As noted before, because of the strong irradiation from the central X-ray source, there should exist a photo-ionized layer at the surface of a cloudlet. The main species of the iron ions in this layer should be in the intermediate-ionization states, e.g. those from Fe^{+18} to $\sim Fe^{+21}$, because in many cases the observed line-centers are around $\sim 6.47 - 6.5$KeV (e.g. Wang et al. 1998; Weaver et al. 2001). Denoting the total number of cloudlets in the whole emission region as $\widetilde{N}$, and the radius

of each cloudlet as r, therefore the covering factor of cloudlets to the central X-ray source is

$$f_c = \frac{\widetilde{N}\pi r^2}{4\pi D^2} = \frac{\widetilde{N} r^2}{4D^2}, \tag{1}$$

which must be less than unity to ensure the central X-ray source to be only partly covered.

From Eq.(1) we see that the unknown quantity $\widetilde{N}r^2$ can be removed by f_c and D. The volume filling factor is

$$f_v = \frac{\widetilde{N}4\pi r^3/3}{4\pi D^3/3} = \widetilde{N}\frac{r^3}{D^3}. \tag{2}$$

Therefore the ratio is $f_v/f_c \approx r/D$, which means that the fractional volume occupied by the cloudlets would be very small if $r \ll D$. At the same time, $\widetilde{N}$ can be still very large to maintain a necessarily large covering factor f_c.

In order to avoid the ambiguity of our quantitative analysis, the following is restricted to calculate the Cerenkov line emission in the optically thick case, though the optically thin case is also possible in AGNs.

The emergent intensity of Cerenkov iron K_α line from the surface of the optically thick dense gas is (Eq. (22) in Appendix, or Eq.(42) in Y00)

$$I_{K_\alpha}^c = Y\left[\ln(1 + X^2) - 2\left(1 - \frac{\arctan X}{X}\right)\right] \quad (\text{ergs/Sec.} \cdot \text{cm}^2 \cdot \text{Str.}), \tag{3}$$

where the parameter $Y \equiv \frac{N_e C_1}{2k_{bf}} \propto N_e$, the density of relativistic electrons; and $X \equiv \sqrt{\frac{k_{bf}}{C_2}}C_0\gamma_c^2 \propto \gamma_c^2 N_{Fe}$, where N_{Fe} and γ_c represent the density of iron ions in gas cloudlets and the typical (or average) energy of the relativistic electrons, respectively. C_0, C_1, C_2 and $k_{bf} \approx k_{bf}(\text{Fe}, \text{L})$ included in X and Y, are the parameters which are dependent on the density N_{Fe} as well as the atomic parameters of concerned ions, e.g. the frequency ν_{lu} (or $h\nu_{lu} \equiv \varepsilon_{lu}$), the transition probability A_{ul}, etc. (Eq. (21) in Appendix or Y00). Inserting the concerned atomic parameters of the iron ions, for iron K_α line, $u = 2$, $l = 1$, we obtain

$$X \equiv \sqrt{\frac{k_{bf}}{C_2}}C_0\gamma_c^2 = 6.49 \times 10^{-28}g_2\sqrt{\frac{S_2}{g_2}\left(\frac{S_1}{g_1} - \frac{S_2}{g_2}\right)}N_{Fe}\gamma_c^2,$$

$$Y \equiv \frac{N_e C_1}{2k_{bf}} = 0.16 \times \frac{g_2}{S_2}\left(\frac{S_1}{g_1} - \frac{S_2}{g_2}\right)N_e, \tag{4}$$

where g_2 and S_2 respectively represent the degeneracy and the real occupation number of electrons at the second level of the iron ion, so $S_2 \leq g_2$. g_1 and S_1 are the corresponding quantities of the first level.

From Eq.(4) we see that in a physically reasonable environment in AGNs, it usually holds that $X < 1$. Therefore Eq.(3) is simplified as

$$I_{K_\alpha}^c \approx YX^2/3, \tag{5}$$

The Cerenkov line emission produced by the thermal relativistic electrons with random direction-distribution of velocities is isotropic, thus the Cerenkov intensity $I^c_{K_\alpha}$ is θ-independent. Therefore the emergent flux $F^c_{K_\alpha}$ from the surface of the dense cloud is simply obtained

$$F^c_{K_\alpha} = 2\pi \int_0^{\pi/2} I^c_{K_\alpha} \cos\theta \sin\theta \mathrm{d}\theta = \pi I^c_{K_\alpha} \quad (\text{ergs/Sec.} \cdot \text{cm}^2). \tag{6}$$

So the elementary luminosity of the Cerenkov iron K_α line of each cloudlet is

$$l^c_{K_\alpha} = 4\pi r^2 F^c_{K_\alpha} = 4\pi^2 r^2 I^c_{K_\alpha} \quad (\text{ergs/Sec.}). \tag{7}$$

Combining Eq.(1) and (7), the total luminosity of Cerenkov iron K_α line from the whole emission region becomes

$$L^c_{K_\alpha} = \tilde{N} l^c_{K_\alpha} = 4\pi^2 r^2 \tilde{N} I^c_{K_\alpha} \approx 16\pi^2 D^2 f_c I^c_{K_\alpha} \quad (\text{ergs/Sec.}). \tag{8}$$

Inserting Eq.(4), (5) into Eq.(8), taking $D \approx 3 \times 10^{15}$cm and $f_c \approx 0.1$, and $S_1 = g_1 = 2$, we obtain

$$L^c_{K_\alpha} = 2.08 \times 10^{-22} \left(1 - \frac{S_2}{g_2}\right)^2 N_e N_{Fe}^2 \gamma_c^4 \quad (\text{ergs/Sec.}), \tag{9}$$

Comparing the Cerenkov luminosity of iron K_α line Eq.(9) with the typical observed value for Seyfert 1s, i. e. $L^{obs.}_{K_\alpha} \approx 10^{40-41}$ ergs/sec., letting $L^c_{K_\alpha} \approx L^{obs.}_{K_\alpha}$, we obtain

$$N_{Fe}^2 \gamma_c^4 N_e \approx 4.8 \times 10^{61} \left(1 - \frac{S_2}{g_2}\right)^{-2} \approx 10^{62}, \tag{10}$$

where for iron ions in intermediate-ionization states, we take $S_2 \approx 1 - 5$, which corresponds to iron ions Fe^{+19}—Fe^{+23}. Eq.(10) gives the combination condition for the iron density N_{Fe}, the density of fast electrons N_e, and the average or typical energy γ_c of the fast electrons to produce the Cerenkov luminosity of iron K_α line which can be compared with the observed value.

Table 1 lists several tentative sets of parameters under the condition, where we arbitrarily fix $N_e = 10^{10}$ cm^{-3}. The choice of combinations is somewhat arbitrary, because so far the environments in AGNs are still not well understood. Some of these parameters may at first appear defiant to the current paradigm around the AGN black holes. In the following section we give discussions on the reasonableness of these parameters and acceptability of the related new scenario around the supermassive black hole in AGNs.

4. Conclusions and Discussions

4.1.In this paper, we tentatively propose another mechanism—the "Cerenkov line-like radiation"—to study the origin of the elusive iron K_α feature in AGNs. The charming advantage

of this new emission mechanism is that the radiation energy of the Cerenkov line is provided by the relativistic electrons rather than by the X-ray continuum. Therefore the continuum and the iron K_α line emission are two components independent of each other. So the lack of correlation between the line and the continuum fluxes can be understood by this way. We further give some model calculations to show the effectiveness of the Cerenkov mechanism to explain the AGNs observations. We show that the calculated Cerenkov iron K_α line is strong enough to compare with observations of AGNs, only if the iron density $N_{\rm Fe}$ in the dense gas, the density of fast electrons $N_{\rm e}$ and the characteristic energy of fast electrons $\gamma_{\rm c}$ are high enough, as shown in Table 1.

If the iron K_α feature indeed arises from the Cerenkov line mechanism, Table.1 signifies the possibility of a strikingly different scenario around the supermassive black hole in AGN—with much denser, more violent and more energetic environs than conventionally believed. In the following 4.2-4.4 sections, we discuss the reasonableness and acceptability of the new scenario.

4.2. Firstly, what are the consequences if there exist abundant relativistic electrons with exceedingly high energies? The problem is in that, except for the Cerenkov line-like radiation, the fast electrons also contribute substantially to the continuum radiation in high energy band through the inverse Compton scattering process (the synchrotron mechanism becomes unimportant in a very dense gas). The Compton power of a fast electron with energy $\gamma_{\rm c}$ passing through an X-rays field with energy density $U_{\rm ph}$ is as high as $p^{\rm Comp.} \approx 2.6 \times 10^{-14} U_{\rm ph} \gamma_{\rm c}^2 \approx 10^{-15} \gamma_{\rm c}^2$ ($U_{ph} \approx 0.1$ ergs/cm^3 for typical Seyfert 1 galaxies). If the density and the energy of the fast electrons are so high as $N_{\rm e} \approx 10^{9-10}$cm^{-3}, and $\gamma_{\rm c} \approx 10^{4-5}$, as shown in Table 1, the Compton luminosity of the continuum in the whole emission region with size $D \sim 10^{15}$cm would be unacceptably higher than the typical observed value $L \approx 10^{44}$ergs/Sec.. Another related problem is that, if both the iron K-line emission and a significant portion of the continuum radiation owing to the inverse Compton scattering process originated from the same group of fast electrons, again the correlation between the fluxes of iron K-line and the X-ray continuum would be expected, as in the case of fluorescence model.

We envisage a solution to overcome the difficulties mentioned above. As pointed out in sec. 3, the fractional volume occupied by the cloudlets, where most of fast electrons reside, can be very small compared with the overall volume of X-ray emission region $V = \frac{4\pi}{3}D^3$, i.e. $f_{\rm v} \ll 1$. In this case, the total number of fast electrons may not be large, thus the corresponding Compton luminosity of the continuum $L^{\rm Comp.} \approx f_{\rm v} \left(\frac{4\pi}{3} D^3 \right) N_e p^{\rm Comp.}$ would be several orders lower than the typical value of the observed continuum luminosity $L \approx 10^{43-44}$ergs/Sec.. A small $f_{\rm v}$ with a large $f_{\rm c}$ is readily realized as long as $r \ll D$, as mentioned in sec. 3. For example, taking $D \sim 10^{15}$ cm, $r \sim 10^{6-7}$ cm, and $f_{\rm c} \sim 0.1$, then the filling factor is small as $f_{\rm v} \sim 10^{-10} - 10^{-9}$, hence we get $L^{\rm Comp.} \ll L^{\rm obs.} \sim 10^{44}$ ergs/Sec..

4.3. Another potential problem concerns the very high density of gas. If $N_{\rm Fe}$ is so high as those shown in Table 1, even up to $\sim 10^{17-18}$ cm^{-3}, and if a cosmological abundance in AGNs is assumed, then the inferred gas density would be inconceivably high. Therefore an abnormally

high iron abundance is necessary to restrict the total gas density at an acceptable level. We envisage two possibilities as follows: either frequent nuclear reactions in the vicinity of the central black hole or a phase transition to form dusty clouds in dense gas regions, could be responsible for the marked increase of abundance of iron and other heavy elements without enhancement of gas density. In the later case, the iron ions may be locked up in tiny grains as embedded impurity. A high density of impurity iron is achievable in a heavily doped solid, even as high as $N_{\mathrm{Fe}} \sim 10^{17-18}$ cm^{-3}. It is conceivable, in principle, that the Cerenkov line-like radiation of iron ions may also occur in the impurity-doped dust, as in gas medium. Undoubtedly, the Cerenkov line-like radiation from the impurity-doped solid would be a challenging problem in experimental physics in future. Existence of dusty clouds with iron-rich grains in the environments of AGNs would be equally mind-boggling in black hole physics.

4.4. Finally, we concern the reasonableness of the energetics of our model. As we suggested in sec.3, the relativistic electrons, necessary for the Cerenkov line-like radiation mechanism, are produced, for example, by the strong shocks, which originate from the mergers processes. However, the energy that goes into the relativistic electron population in this way could only be a small fraction of the total. In this case, it would be important to give a more comprehensive physical consideration on the 'efficiency of energy transformation from the kinetic energy of shock to the thermal energy of relativistic electrons'. We hope to give a moderate solution in future.

REFERENCES

Boller Th., Fabian A. C., Sunyaev R., Trumper J., Vaughan S., Ballantyne D. R., 2002, MNRAS, 329, 1

Brandt W. N., Gallagher S. C., 2000, New Astronomy Reviews, 44, 461

Celotti A., Fabian A. C., Rees M. J., 1992, MNRAS, 255, 419

Chiang J., et al., 2000, ApJ, 528, 292

Collin-Souffrin S., Czerny B., Dumont A. M., Zycki P. T., 1996, A&A, 314, 393

Done C., Madejski G. M., Zycki P. T., 2002, ApJ, 536, 213

Fabian A. C., Rees M. J., Stella L., White N. E., 1989, MNRAS, 238, 729

Fabian A. C., Vaughan S., Nandra K., Iwasawa K., Ballantyne D. R., Lee J. C., De Rosa, A., Turner A., Young A. J., 2002, MNRAS, 335, L1

Guilbert P. W., Rees M. J., 1998, MNRAS, 233, 475

Karas V., Czerny B., Abrassart A., Abramowicz M. A., 2000, MNRAS, 318, 547

Kuncic Z., Blackman E. G., Rees M. J., 1996, MNRAS, 283, 1322

Kuncic Z., Celotti A., Rees M. J., 1997, MNRAS, 284, 717

Lee J., Fabian A. C., Brandt W. N., Reynolds C. S., Iwasawa K., 1999, MNRAS, 310, 973

Lee J., Fabian A. C., Reynolds C. S., Brandt W. N., Iwasawa K., 2000, MNRAS, 318, 857

Lightman A. P., White T. R., 1998, ApJ, 335, 57

Malzac J., 2001, MNRAS, 325, 1625

Meszaros,P., 2002, ARA&A, 40, 137

Miniutti G., Fabian A. C., Goyder R., Lasenby A. N., 2003, MNRAS (preprint astro-ph/0307163)

Nandra K., George I. M., Mushotzky R. F., Turner T. J., Yaqoob T., 1997a, ApJ, 477, 602; 1997b, ApJ, 488, 91

Piran T., 1999, Physics Reports, 314, 575

Rees M. J., 1987, MNRAS, 228, 47

Reynolds C. S., 2001, ASP Conf. Series Vol. TBD, p105

Sulentic J. W., Marziani P., Calvani M., 1998a, ApJ, 497, L65

Sulentic J. W., Marziani P., Zwitter T., Calvani M., Dultzin-Hacyan D., 1998b, ApJ, 501, 54

Tanaka, Y et al., 1995, Nature, 375, 659

Vaughan S., Fabian A. C., Nandra K., 2003, MNRAS, 339, 1237

Wang T. G., Otani C., Cappi M., Leighly K. M., Brinkmann W., Matsuoka M., 1998, MNRAS, 293, 397

Wang J. X., Wang T. G., Zhou Y. Y., 2001, ApJ, 549, 891

Wang J. X., Zhou Y. Y., Xu H. G., Wang T. G., 1999, ApJ, 516, 65

Weaver K. A., Gelbord J., Yaqoob T., 2001, ApJ, 550, 261

Xu K., Z., Yang B. X., Xi F. Y., 1981, Phys. Lett. A86, 24

Xu K., Z., Yang B. X., Xi F. Y., 1988, Phys. Rev. A33, 2912

Xu K., Z., Yang B. X., Xi F. Y., 1989, Phys. Rev. A40, 5411

You J. H., Xu Y. D., Liu D. B., Shi J. R., Jin G. X., 2000, A&A, 362, 762

You J. H., Cheng F. H., 1980, Acta Phys. Sinica, 29, 927

You J. H., Cheng F. H., Cheng F. Z., Kiang T., 1986, Phys. Rev. A34, 3015

Appendix: Basic Formulae for Cerenkov line-like radiation

We first emphasize that the CGSE system of units was used in the Appendix. This means, in particular, that all energies of X-ray photons in the following formulae will be in ergs rather than KeV (1 KeV=1.602×10^{-9} erg). Besides, one can find the detailed derivation of the following basic formulae in our published paper (You et al. 2000).

1. The refractive index n and the extinction coefficient κ

The essential point of the calculation of the spectrum of Cerenkov radiation is the evaluation of the refractive index of the gaseous medium. This is easy to understand qualitatively from the necessary condition for producing Cerenkov radiation, $v > c/n_\nu$. At a given frequency ν, the larger the index n_ν, the easier the condition $v > c/n_\nu$ to be satisfied, and the stronger the Cerenkov radiation at ν will be. Therefore, in order to get the theoretical spectrum of Cerenkov radiation, it is necessary to calculate the refractive index n_ν and its dependence on ν (the dispersion curve $n_\nu \sim \nu$). For a gaseous medium, the calculation is easy to do. Omitting the detailed derivation, here we only give the expressions of the index n_ν and the extinction coefficient κ_ν of gas as follows

$$n_\nu^2 - 1 = \frac{C^3 h^4}{16\pi^3} \varepsilon_{lu}^{-4} A_{ul} g_u N_{\text{Fe}} \left(\frac{S_l}{g_l} - \frac{S_u}{g_u} \right) y^{-1}$$

$$\kappa_\nu = \frac{C^3 h^4}{128\pi^4} \varepsilon_{lu}^{-5} \Gamma_{lu} A_{ul} g_u N_{\text{Fe}} \left(\frac{S_l}{g_l} - \frac{S_u}{g_u} \right) y^{-2} \quad \text{(when } y \geq 10^{-5}) \quad (11)$$

where $\varepsilon_{ul} \equiv h\nu_{ul} = \varepsilon_u - \varepsilon_l$ represents the energy of line photon, ε_u and ε_l are the energy of the upper and lower levels of the iron ion, respectively (for definiteness, in the following, we only concern with the Cerenkov iron line, particularly the iron K$_\alpha$). A_{ul} is the Einstein's spontaneous emission coefficient for $u \to l$. $\Gamma_{ul} = \Gamma_u + \Gamma_l = \sum_{i<u} A_{ui} + \sum_{j<l} A_{lj}$ is the quantum damping constant for the atomic(ionic) line with energy ε_{ul}, which is related with the Einstein's spontaneous emission probabilities A_{ui} and A_{lj}. N_{Fe} is the number density of iron ions in gas. g_u (or g_l), and S_u (or S_l) are the degeneracy and the actual occupation number of electrons of the upper level u (or lower level l), respectively. $y \equiv \frac{\Delta\lambda}{\lambda_{ul}} = -\frac{\Delta\nu}{\nu_{ul}} = -\frac{\Delta\varepsilon}{\varepsilon_{ul}} = \frac{\varepsilon_{lu}-\varepsilon}{\varepsilon_{lu}}$ represents the fractional displacement of the frequency or photon-energy. $y \ll 1$ owing to the fact that Cerenkov line-like radiation concentrates in a narrow band $\varepsilon \approx \varepsilon_{ul}$.

2. The Cerenkov spectral emissivity J_ν^c (or J_ε^c)

The Cerenkov spectral emissivity can be derived from the dispersion curve $n_\nu \sim \nu$ given above. It is known from the basic theory of Cerenkov radiation that the power emitted in a frequency interval $(\nu, \nu + d\nu)$ or $(\varepsilon, \varepsilon + d\varepsilon)$ by an electron moving with velocity $\beta = \frac{v}{c}$ is $P_\nu d\nu = (4\pi^2 e^2 \beta\nu/c)(1 - \frac{1}{n_\nu^2 \beta^2})d\nu$. Let $N(\gamma)d\gamma$ to be the number density of fast electrons in the

energy interval $(\gamma, \gamma + d\gamma)$ ($\gamma \equiv \frac{1}{\sqrt{1-\beta^2}} = \frac{mc^2}{m_0c^2}$ is the Lorentz factor, representing the dimensionless energy of the electron). For an isotropic velocity distribution of the relativistic electrons as in normal astrophysical conditions, the Cerenkov radiation will also be isotropic. Then the Cerenkov spectral emissivity $J_\nu^c d\nu$, or equivalently, $J_y^c dy = J_\nu^c d\nu$, can simply be obtained by the integral $J_\nu^c d\nu = \frac{1}{4\pi} \int_{\gamma_1}^{\gamma_2} N(\gamma) d\gamma P_\nu d\nu$, thus we get

$$J_y^c \mathrm{d}y = C_1 N_e (y^{-1} - y_{\lim}^{-1}) \mathrm{d}y \tag{12}$$

where N_e is the density of fast electrons. $y \equiv -\frac{\Delta\varepsilon}{\varepsilon_{ul}}$ is the fractional displacement of energy ε relative to intrinsic line-energy $\varepsilon_{ul} \equiv h\nu_{ul}$. $y_{lim} = C_0 \gamma_\mathrm{c}^2$ is the fractional Cerenkov line-width. C_0, C_1 are the coefficients which are dependent on the density of iron ions N_Fe and the atomic parameters of concerned species of iron ions, as shown below.

3. The absorption coefficient

For an optically thick dense gas for which the Cerenkov line mechanism is more efficient, the final emergent intensity I_ν^c is dertermined by the competition between the emission J_ν^c (or J_ε^c) and the absorption k_ν. Therefore it is necessary to consider the absorption of the gas at $\nu \approx \nu_{lu}$. For the optical and X-ray bands, only two absorption mechanisms are important for the Cerenkov line. One is the line absorption k_{lu} in the vicinities of atomic lines, which directly related to the extinction coefficient κ_ν given in Eq. (11) by a simple relation, i. e. $k_{lu} = 4\pi\nu\kappa_\nu/c$. Another is the photoelectric absorption k_bf. The free-free absorption in X-ray band is negligibly small. Thus the total absorption is

$$k_\nu = k_{lu} + k_\mathrm{bf} = C_2 y^{-2} + k_\mathrm{bf} \tag{13}$$

where the coefficient C_2 depends on N_Fe and other atomic parameters, as C_0, C_1 does. Owing to the fact that the line absorption decreases with $\Delta\nu = \nu - \nu_{lu}$ rapidly as $k_{lu} \propto y^{-2}$, $k_{lu}(\nu < \nu_{lu}) \to 0$. Therefore in the whole actually effective frequency band of Cerenkov line emission, the dominant absorption is k_bf. Particularly, for iron $K\alpha$ line which we concern, the dominant photoelectric absorbers are the L-shell electrons of iron ions. In this case, Eq.(13) becomes

$$k_\nu = k_{lu} + k_\mathrm{bf} \approx k_\mathrm{bf} \approx k_\mathrm{bf}(Fe, L) \tag{14}$$

and

$$k_\mathrm{bf}(Fe, L) = N_\mathrm{Fe} S_2 \sigma_\mathrm{bf}(2) \tag{15}$$

where S_2 is the occupation number of electrons in L-shell, thus $S_2 \leq g_2 = 8$. $\sigma_\mathrm{bf}(2)$ is the cross section of photoelectric absorption of a L-shell electron. For an iron atom or ion, the hydrogen-like formula for the cross section is a good approximation, particularly for the low-lying levels n=2, 3, i.e.

$$\sigma_\mathrm{bf}(\nu, n) = \frac{32\pi^2 e^6 R_\infty Z^4}{3\sqrt{3}h^3\nu^3 n^5} g_\mathrm{bf}(\nu, T) \tag{16}$$

Inserting to Eq.(15), taking the effective charge number $Z^{\text{eff.}} = 24$ for the L-shell electrons at level $n = 2$, and let Gaunt factor $g_{\text{bf}} \approx 1$, we get

$$k_{\text{bf}}(\text{Fe, L}) \approx 8.4 \times 10^{-46} N_{\text{Fe}} S_2 \varepsilon_{lu}^{-3} \tag{17}$$

4. The emergent Cerenkov spectral intensity and Cerenkov total line intensity

For an uniform plan-parallel slab, the emergent Cerenkov spectral intensity I_ν^c from the surface of the slab can be derived by use of the equation of radiative transfer

$$I_\nu^c = \frac{J_\nu^c}{k_\nu}(1 - e^{-k_\nu L}) \tag{18}$$

where J_ν^c and k_ν (or J_y^c and k_y) are given by Eq. (12) and (13), respectively.

For optically thin gas, $\tau_\nu = k_\nu L \ll 1$, therefore the Cerenkov line intensity is

$$I_\nu^c \approx J_\nu^c L \tag{19}$$

However, for a very dense gas, the Cerenkov emission slab becomes optically thick, thus Eq.(18) can be simplified as $I_\nu^c \approx \frac{J_\nu^c}{k_\nu}$, or equivalently,

$$I_y^c = \frac{J_y^c}{k_{lu} + k_{\text{bf}}} = \frac{N_e C_1 (y^{-1} - y_{lim}^{-1})}{C_2 y^{-2} + k_{\text{bf}}} \tag{20}$$

where $y_{lim} = C_0 \gamma_c^2$ is the fractional Cerenkov line width. All of the atomic parameter-dependent coefficients C_0, C_1, C_2, k_{bf} for iron ions are given as follows.

$$C_0 = 1.05 \times 10^{-76} \varepsilon_{lu}^{-4} A_{ul} g_u N_{\text{Fe}} \left(\frac{S_l}{g_l} - \frac{S_u}{g_u} \right)$$

$$C_1 = 5.77 \times 10^{-53} \varepsilon_{lu}^{-2} A_{ul} g_u N_{\text{Fe}} \left(\frac{S_l}{g_l} - \frac{S_u}{g_u} \right)$$

$$C_2 = 1.75 \times 10^{-87} \varepsilon_{lu}^{-4} A_{ul} \Gamma_{lu} g_u N_{\text{Fe}} \left(\frac{S_l}{g_l} - \frac{S_u}{g_u} \right)$$

$$k_{\text{bf}}(\text{Fe, L}) = 8.4 \times 10^{-46} \varepsilon_{lu}^{-3} S_2 N_{\text{Fe}} \text{ (only for iron K} - \text{lines)} \tag{21}$$

For iron K_α line, $u = 2$, $l = 1$. We emphasize again that the photon energy ε_{lu} in Eqs. (21) is in units erg (the CGSE units) rather than KeV (1 KeV=1.602×10^{-9} ergs). Eq.(20) gives a broad and asymmetric profile of Cerenkov line with a small Cerenkov line-redshift, as shown in Fig.3.

Inserting Eq.(20) into the integral $I^c = \int_0^{y_{lim}} I_y^c dy$, we obtain the total line intensity I^c in optically thick case

$$I^c = Y \left[\ln(1 + X^2) - 2 \left(1 - \frac{\arctan X}{X} \right) \right] \qquad (\text{erg/sec.} \cdot \text{cm}^2 \cdot \text{str.}) \tag{22}$$

where $Y \equiv \frac{N_e}{2} \frac{C_1}{k_{\mathrm{bf}}} \propto N_e$, N_e is the density of relativistic electrons. $X \equiv \sqrt{\frac{k_{\mathrm{bf}}}{C_2}} C_0 \gamma_c^2 \propto \gamma_c^2 N_{\mathrm{Fe}}$, N_{Fe}, γ_c represent the density of iron ions in gas and the typical energy of relativistic electrons, respectively. Therefore the total Cerenkov line intensity I^c is determined by the parameters N_e, N_{Fe}, and γ_c. Inserting the atomic parameters of iron ions into Eq.(21), for the iron $K\alpha$ line, we obtain

$$X = 6.49 \times 10^{-28} g_2 \sqrt{\frac{S_2}{g_2} \left(\frac{S_1}{g_1} - \frac{S_2}{g_2} \right)} N_{\mathrm{Fe}} \gamma_c^2$$

$$Y = 0.16 \times \frac{g_2}{S_2} \left(\frac{S_1}{g_1} - \frac{S_2}{g_2} \right) N_e \tag{23}$$

From eq. (23) we see, in a physically reasonable environment of AGNs, we usually have $X < 1$, or equivalently, $N_{\mathrm{Fe}} \gamma_c^2 < 10^{27}$, Therefore, for optically thick and $X < 1$ case, Eq. (22) is simplified as

$$I_{K\alpha}^c \approx \frac{1}{3} Y X^2 \tag{24}$$

X, Y are given by Eq.(23) for iron K_α line. In another extremely case, $X > 1$, or equivalently, $N_{\mathrm{Fe}} \gamma_c^2 > 10^{27}$, Eq.(22) is simplified as

$$I_{K\alpha}^c \approx 2Y (\ln X - 1) \approx 2Y \qquad \text{for X > 1 case} \tag{25}$$

Table 1: Combinations of Iron Density, Characteristic Energy and Density of Relativistic Electrons for Calculation of Cerenkov Luminosity of Iron K_α Line

$N_{\mathrm{Fe}}(\mathrm{cm}^{-3})$	γ_c	$N_e(\mathrm{cm}^{-3})$
10^{14}	10^6	10^{10}
10^{15}	3×10^5	10^{10}
10^{16}	10^5	10^{10}
10^{17}	3×10^4	10^{10}
10^{18}	10^4	10^{10}
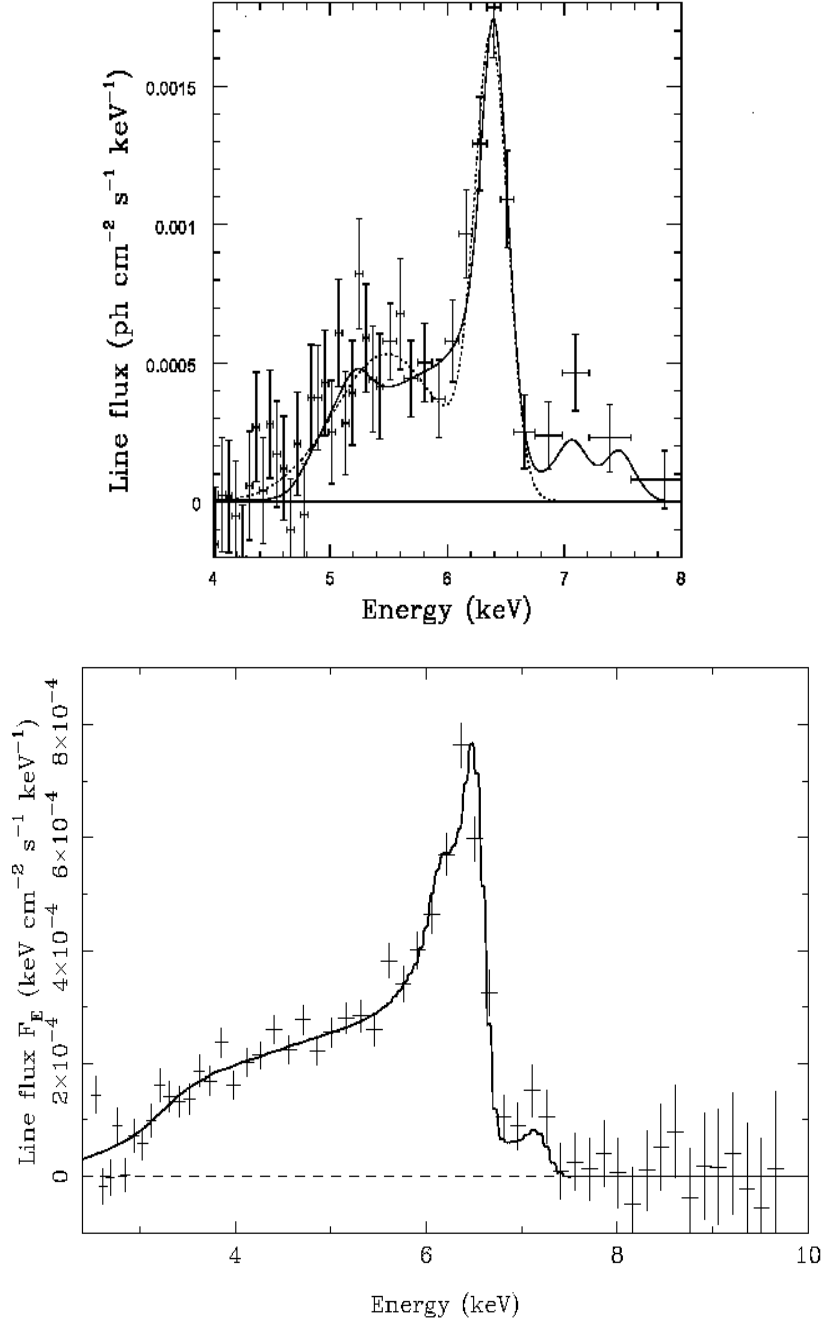
Fig. 1.— The observed iron K_α line of Seyfert 1 galaxy NGC 4151(upper panel,taken from Wang et al. 2001) and MCG-6-30-15(lower panel, taken from Fabian et al. 2002). The small line-like hump at $\sim$7-8KeV(in rest frame) is due to the iron K_β line emission.
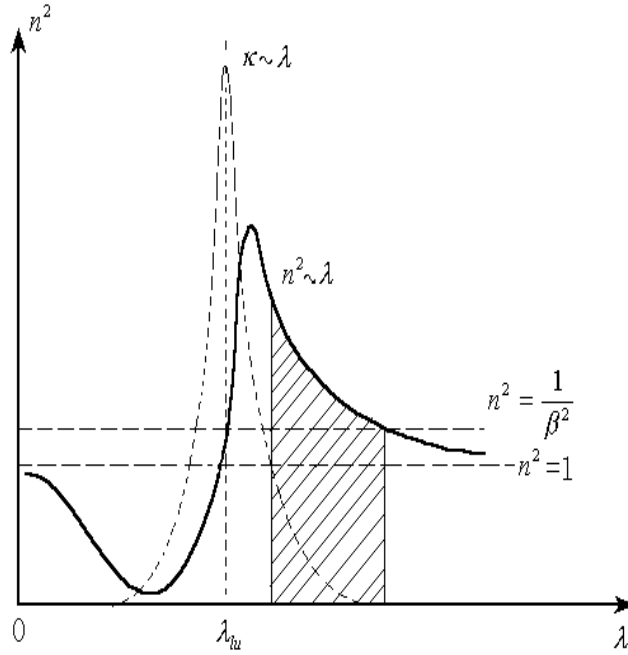
Fig. 2.— Schematic sketch of the dispersion curve of gas $n^2 \sim \lambda$, and the curve $\kappa \sim \lambda$, where κ is the extinction coefficient of gas, which relates with the line-absorption coefficient by a simple formula $k_\lambda = \frac{4\pi}{\lambda}\kappa_\lambda$. The Cerenlov radiation survives in the shaded narrow region where the Cerenkov radiation condition $n \geq 1/\beta$ is satisfied, and where the extinction is small. The shaded region is narrow, making the emerging radiation appear more like a line emission than a continuum.
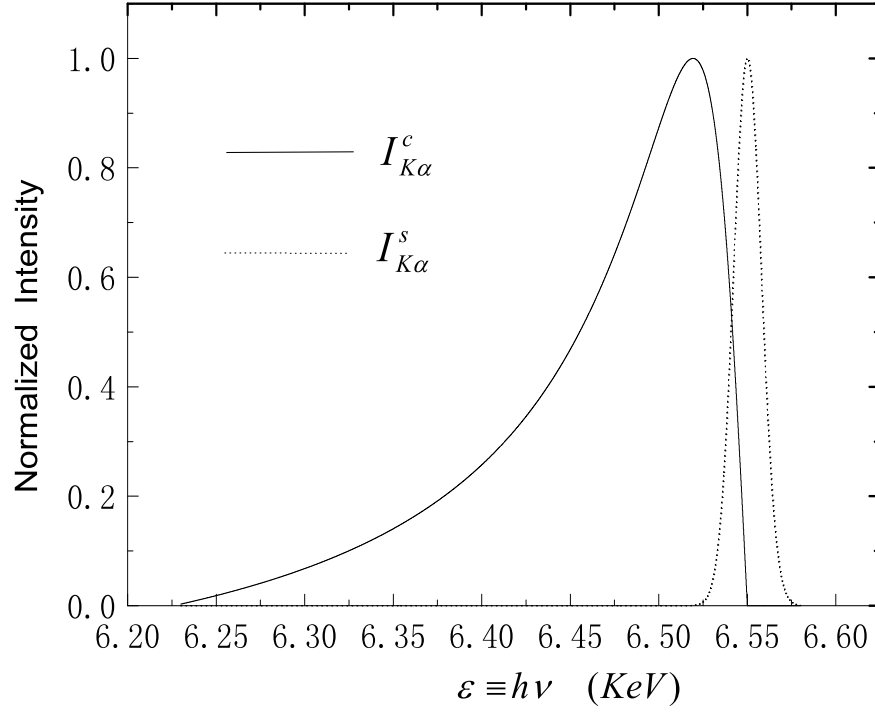
Fig. 3.— The calculated profile of Cerenkov line $I^c_{K_\alpha} \sim \varepsilon$ of iron ion Fe^{+21} in optically thick case, assuming $N_{Fe} = 10^{17} cm^{-3}$ and $\gamma_c = 2 \times 10^5$, where $\varepsilon \equiv h\nu$ is the energy of line photon. The Cerenkov line-profile is broad, asymmetric, and redshifted. The profile of a normal line by spontaneous transition $I^s_{K_\alpha} \sim \varepsilon$ is also plotted for comparison.
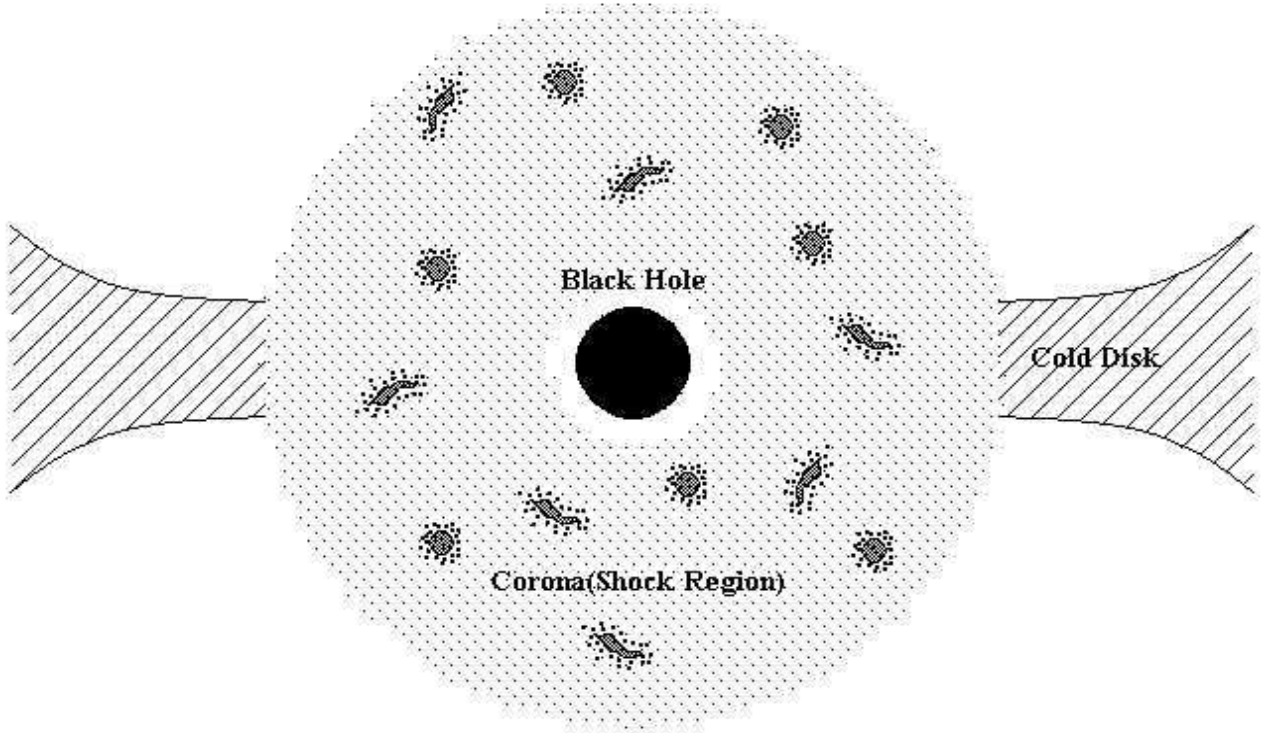
Fig. 4.— Schematic sketch of the emission region of iron K_α line around a central supermassive black hole of AGN. The shaded circles or strips represent cloudlets or filaments consist of cold dense gas. The dotted region is the hot, rarified corona where the tiny dots and the black dots represent thermal electrons and relativistic electrons, respectively. The thermal electrons have an uniform distribution but the relativistic electrons have a high concentration around the clouds and/or filaments.